J Mater Sci (2012) 47:4200–4204
DOI 10.1007/s10853-011-6185-1

LETTER

Complex impedance analysis on a layered perovskite-like ceramic: $La_3Ti_2TaO_{11}$

Chunchun Li · Xiaoyong Wei

Received: 24 October 2011 / Accepted: 6 December 2011 / Published online: 28 December 2011

Introduction

Ac-impedance analysis is a very convenient and powerful technique to study the electrical properties of polycrystalline materials and to correlate the electrical properties with their microstructure. One of the strengths of ac-impedance analysis is that it helps us to separate the contributions of grains from other impedance components, such as grain boundary, interfaces, electrodes, etc. [1–6]. The impedance measurements of a material give us data including real part and imaginary part components. Data may be analyzed in terms of four possible complex formalisms: the impedance Z^*, the electric modulus M^*, the admittance Y^*, and the permittivity ε^*. These are interrelated in accordance with the relation:

$$M^* = j\omega C_0 Z^* \quad (1)$$

$$\varepsilon^* = (M^*)^{-1} \quad (2)$$

$$Y^* = (Z^*)^{-1} \quad (3)$$

$$Y^* = j\omega C_0 \varepsilon^* \quad (4)$$

where ω is the angular frequency ($\omega = 2\pi f$); and C_0 is the capacitance of vacuum. Results may be presented in various ways, e.g., as complex plane plots (real *vs* imaginary,) or as spectroscopic plots (real and/or imaginary against frequency). In addition, recently, it has been suggested that combined impedance and modulus spectroscopy plots offer the possibility of a comprehensive characterization of electronic microstructure since the combined impedance and modulus spectroscopy plots give information that is not immediately apparent from either analysis in isolation [7–11].

In recent years, the perovskite-like-structured (PLS) ferroelectrics with a formula of $A_nB_nO_{3n+2}$ ($n = 2 \sim 7$) have received considerable attention in view of their wide-ranging properties, such as dielectric, ferroelectric, piezoelectric, magnetic, electro-optic, microwave properties, and superconducting properties [12–17]. The diverse properties of $A_nB_nO_{3n+2}$ are related to their unique structure composed of corner-shared BO_6 octahedra with A cations within the perovskite-like layers, where n is the number of octahedral layers in the perovskite slab [12, 13, 16]. $La_3Ti_2TaO_{11}$ is a member of the family of $A_nB_nO_{3n+2}$ with $n = 3$. It was studied with regard to its synthesis through various methods, and detailed structural characterization using X-ray diffraction [18, 19] revealed that $La_3Ti_2TaO_{11}$ crystallized in orthorhombic symmetry with space group $Pmc2_1$. A detailed literature survey revealed that the electrical properties of $La_3Ti_2TaO_{11}$ have not been reported. In this study, we prepared crystalline $La_3Ti_2TaO_{11}$ ceramics using solid-state ceramic route, and the electrical properties of $La_3Ti_2TaO_{11}$ ceramics were investigated by ac-impedance analysis.

Experimental procedure

$La_3Ti_2TaO_{11}$ samples were prepared by high-temperature solid-state reactions of high-purity raw powders of La_2O_3 (99.9%), Ta_2O_5 (99.95%), and TiO_2 (99.9%). Stoichiometric amounts of the raw powders were weighed and ball

C. Li · X. Wei (✉)
Electronic Materials Research Laboratory, Key Laboratory of the Ministry of Education, Xi'an Jiaotong University, Xi'an 710049, People's Republic of China
e-mail: wdy@mail.xjtu.edu.cn

C. Li · X. Wei
International Center for Dielectric Research, Xi'an Jiaotong University, Xi'an 710049, People's Republic of China

milled using zirconia balls for 4 h in plastic containers with ethanol as media. The powders were calcined at 1350 °C for 4 h. They were then remilled well and mixed with 5 wt.% solution of PVA as a binder. The resultant powders were then uniaxially pressed into cylindrical disks with 11-mm diameter and 1–2-mm height under a pressure of 150 MPa. The samples were fired at 600 °C for 2 h to remove the organic binder and then sintered in the range of 1480–1560 °C for 4 h. The samples were cooled at a rate of 2 °C/min to 1100 °C, and then naturally cooled to room temperature. The as-sintered $La_3Ti_2TaO_{11}$ disks were then annealed at 1200 °C for 10 h.

The densities of the compacts were measured by the Archimedes method. The phase constitution of the samples was examined using an X-ray diffractometer (Rigaku D/MAX-2400, Japan) using CuKa radiation ($\lambda = 0.154$ 06 nm) in a 2θ range from 15 to 55°. The microstructures were studied using a JEOL JSM-6390A scanning electron microscopy (SEM). Impedance measurements were carried out using HP 4284 LCR meter equipped in the frequency range from 100 Hz to 1 MHz with a thermostat from room temperature (20 °C) to 800 °C. Before the measurements, electrodes were fabricated on opposite pellet faces from Pt paste which was dried, decomposed, and hardened by gradually heating to 900 °C.

Results and discussion

XRD pattern performed on the $La_3Ti_2TaO_{11}$ ceramic sintered at 1540 °C is presented in Fig. 1. All the peaks could be indexed based on JCPDS file number of 54-0632 for $La_3Ti_2TaO_{11}$ with space group $Pmc2_1$. This suggested that the as-sintered product was definitely single-phase ceramic.

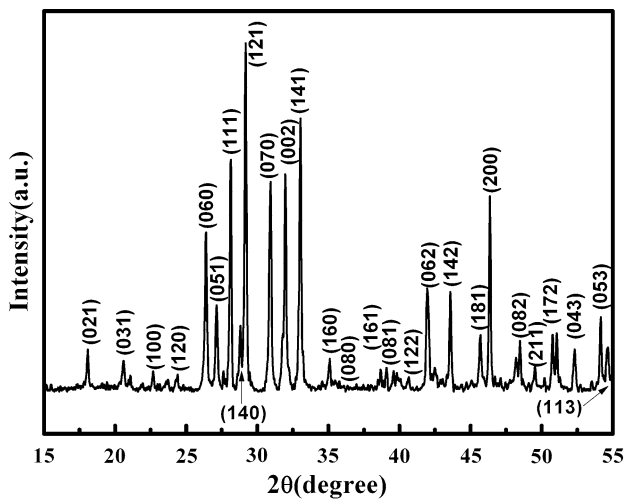

Fig. 1 Room-temperature XRD patterns of $La_3Ti_2TaO_{11}$ sample sintered at 1540 °C

Dense ceramics with relative densities above 90% were obtained when sintered above 1510 °C. Fig. 2a–c presents SEM images obtained for the thermally etched surface of $La_3Ti_2TaO_{11}$ ceramics sintered at different temperatures. A porous microstructure was observed for the 1480 °C-sintered ceramic (Fig. 2a). With increasing sintering temperature, the grain size of the ceramics was slightly increased, while the porosity decreased. When sintered at 1540 °C, a dense microstructure with an average grain size of 2–5 μm was formed (Fig. 2d).

Figure 3 shows the frequency dependence of real part of impedance (Z') at different temperatures from 500 to 800 °C. It was observed that Z' values decreased gradually with increasing frequency, indicating the conductivity increased with frequency. In low-frequency region ($f < 10$ kHz), there was a dispersion in Z' value for different temperatures. In contrast, the curves approached each other at high-frequency irrespective of the temperature. This might be related to the release of space charges resulted from the reduction of barrier potential in materials with increasing temperature. Besides, at low frequencies, Z' value increased with increasing temperature up to 600 °C, and thereafter it decreased with further increase in temperature. This result implied that there might be a positive temperature coefficient of resistance (PTCR) effect in the present samples.

Figure 4 shows the variation of the imaginary part of impedance (Z'') as a function of frequency at different temperatures. Z'' value reached a maximum at a characteristic frequency for a fixed temperature. Broad peaks with slight asymmetry in Z''–log (f) plots were observed at characteristic frequencies, where Z'' reached maximum values. The characteristic frequency exhibited strong temperature dependence: it shifted toward the low-frequency side with increasing temperature up to 600 °C, and thereafter it shifted toward the higher frequency. Further, the magnitude of Z'' increased with increasing temperature up to 600 °C, and subsequent increase in measurement temperature decreased the Z'' value. The variation of the magnitude of Z'' value with measurement temperature might be related to the fact that there existed PTCR effect in the present samples.

The complex impedance plane plots measured at various temperatures in the range of 500–800 °C are shown in Fig. 5. Only a single, semicircular arc in the impedance complex plane was observed for a fixed temperature. These results suggested that the samples might be represented by a simple, single parallel RC element. It is, however, well known that the polycrystalline ceramics consist of randomly oriented grains separated by grain boundaries, resulting in the heterogeneity in electrical properties. This information made us to query the simple representation of the complex impedance plane plots of $La_3Ti_2TaO_{11}$ samples.

To get a comprehensive characterization of electronic microstructure, a combination of spectroscopic plots of the

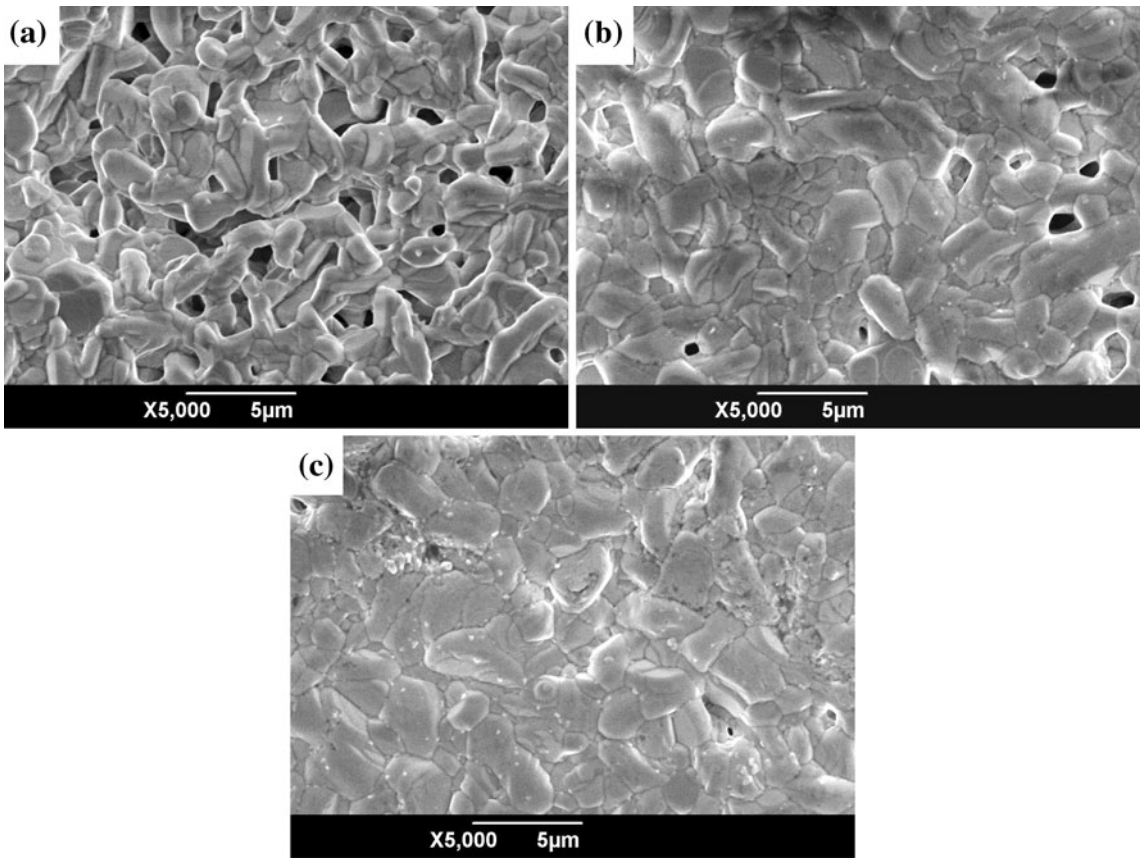

Fig. 2 SEM of $La_3Ti_2TaO_{11}$ sintered at: **a** 1480 °C. **b** 1510 °C. **c** 1540 °C

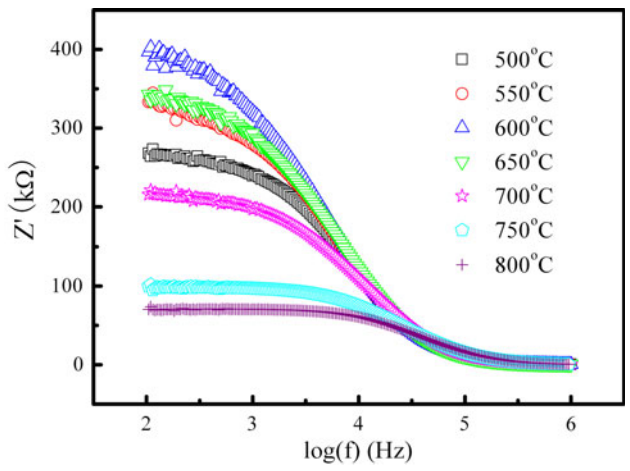

Fig. 3 The frequency dependence of real part of impedance (Z') at different temperatures

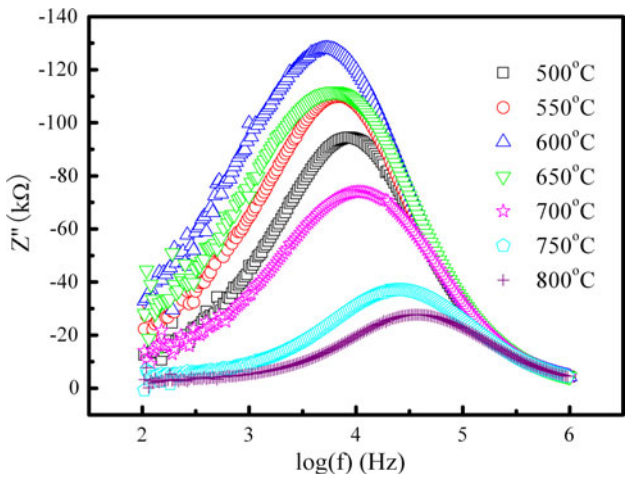

Fig. 4 The variation of the imaginary part of impedance (Z'') as a function of frequency at different temperatures

imaginary part of the impedance, Z'', and modulus, M'', measured at 600 °C, was shown in Fig. 6. The spectroscopic plots showed a similar effect with a single peak in both Z''–f and M''–f plots. Nevertheless, the separation of peak maxima was clear. By comparing the equations for the imaginary parts of the impedance (Z''), and modulus (M'') for a simple parallel RC element, [2, 4]:

$$Z'' = R \cdot \frac{\omega CR}{1 + (\omega CR)^2} \tag{5}$$

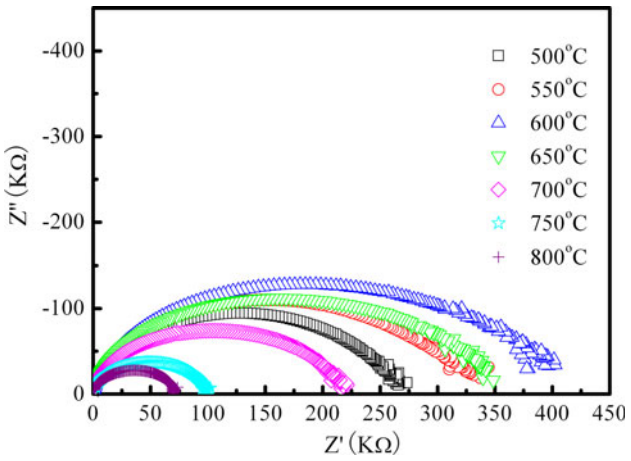

Fig. 5 The complex impedance plane plots measured at various temperatures in the range 500–800 °C

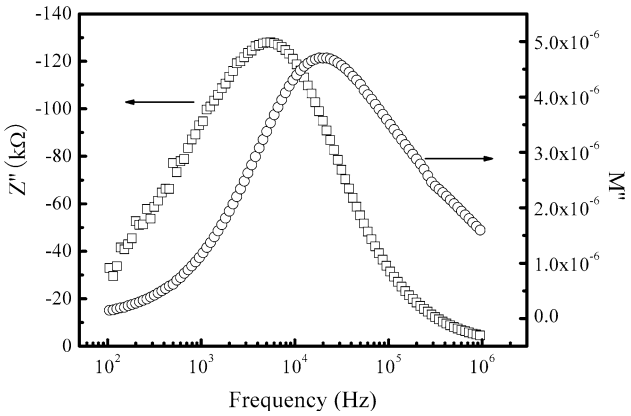

Fig. 6 The combined impedance and modulus spectroscopy plots at 600 °C

$$M'' = \frac{\omega CR}{1 + (\omega CR)^2} \cdot \frac{C_0}{C} \tag{6}$$

we could see that both *Z''* and *M''* approached their maxima when ωCR was equal to 1. Therefore, the peak of *Z''*–*f* plot should coincide with that of *M''*–*f* plot for a same parallel *RC* element. Thus, the separation of their peaks indicates the existence of additional impedance response in the present system. Previous report [1] revealed that the impedance plots gave the most emphasis to the most resistive components in samples and thus the associated peak and semicircle of the elements with much smaller resistance disappeared from the impedance plots. In addition, it was reported that the grain size was a major factor influencing the electrical properties. As the grain size becomes smaller, the number of semicircles in the complex impedance plots can be reduced [20–22]. Ponpandian et al. [21] reported that samples of larger grains showed two semicircles, while the nanocrystalline $NiFeO_4$ samples with smaller grain size showed only one semicircle ascribed to the grain boundary conduction. It is worthy to note that the average grain size of the present ceramics are around 3–5 μm (as shown in Fig. 2). Therefore, we conclude that the much smaller resistance of grains and the small grain size of the $La_3Ti_2TaO_{11}$ gave rise to the simple impedance response.

The overall resistances (R_T) of the sample were extracted from the intercepts on the real part of *Z* (*Z'*) axis variations of which with temperature are shown in Fig. 7. It could be observed that the resistance increased with increasing measurement temperature up to 600 °C when it reached a maximum value, while subsequent increase in temperature decreased the resistance. This confirmed the existence of PTCR effect. Further, researches are in progress to explain the PTCR effect. The capacitance values were calculated from the frequency peaks of the semi-circular arcs using the relation $\omega CR = 1$. A. R. West et al. [1] established a relation between the magnitudes capacitance values and their possible response, which could be used to diagnose bulk, grain boundary, surface layer, and electrochemical phenomena. The calculated capacitance values were in the order of 10^{-10} F. This result indicated the nature of the semicircle to be due to the grain boundary.

A more conventional method of presenting resistance (or conductivity) data is an Arrhenius plot against reciprocal temperature. The ac conductivity of the material is evaluated in accordance with the relation:

$$\sigma_{ac} = \omega \varepsilon_0 \varepsilon_r \tan\delta = 2\pi f \varepsilon_0 \varepsilon_r \tan\delta \tag{7}$$

The *ac* conductivity values of $La_3Ti_2TaO_{11}$ ceramic observed at different frequencies are shown in Fig. 8 as a function of temperature. It could be seen that the ac conductivity showed a progressive rise with increasing temperature with different slopes at different temperature regions. In low-temperature region, the variation of ac conductivity with temperature was smooth, accompanied

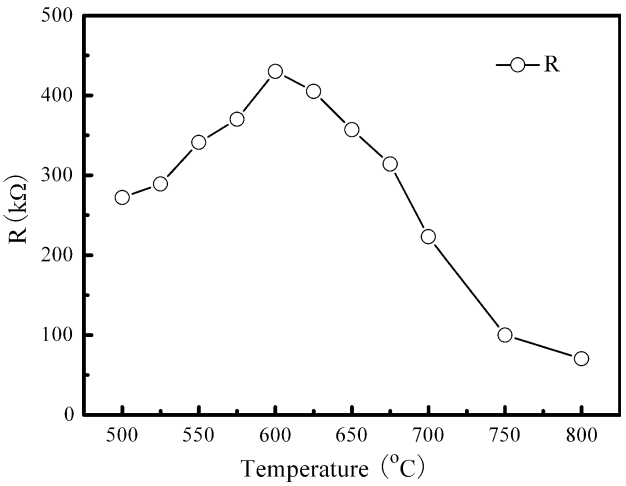

Fig. 7 Temperature dependence of resistances in $La_3Ti_2TaO_{11}$

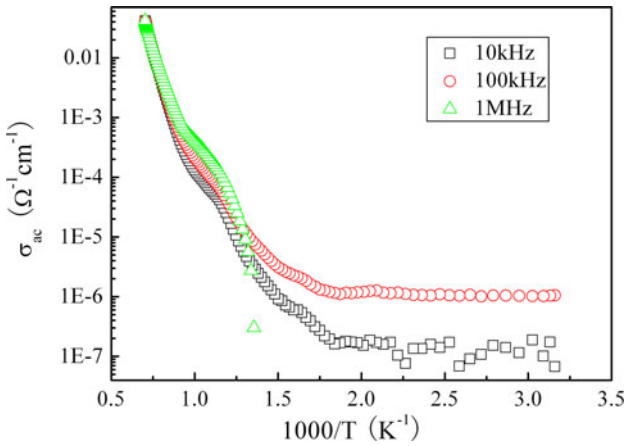

Fig. 8 The ac conductivity of $La_3Ti_2TaO_{11}$ ceramic observed at different frequencies as a function of temperature

with strong frequency dispersion in σ_{ac} value. As temperature rises to 900 °C, the slope increased steeply until it reached a maximum value of 0.04 Ω^{-1} cm^{-1} (10 kHz), which was much higher compared with room temperature value of 6.75 × 10^{-8} Ω^{-1} cm^{-1}(10 kHz). σ_{ac} value merges finally in the high temperature region. In addition, the higher conductivity was observed at higher frequencies in the low-temperature region. These results indicated that the electrical conduction in the present material was a thermally activated process related to the release of space charge, which was in very good agreement with the impedance analysis results. A similar effect [23] was previously observed in $LaLiMo_2O_8$. σ_{ac} value at 1 MHz could not be obtained when measured below 500 °C because the dielectric loss ($tan\delta$) was of negative value. This may be attributed to the low loss of the as-prepared $La_3Ti_2TaO_{11}$ ceramics.

Conclusions

Complex impedance analysis was carried out on polycrystalline $La_3Ti_2TaO_{11}$ ceramics synthesized by solid-state ceramic route. A preliminary structural analysis indicated the crystal structure to be orthorhombic with space group $Pmc2_1$. Impedance spectrum results indicated that the electrical properties of the material were strongly dependent on frequency and temperature. Only a single semicircle was observed in complex impedance plane plots for a fixed temperature. This could be explained by the small grain size of $La_3Ti_2TaO_{11}$, which was well agreement with the SEM results. A PTCR effect was observed in temperature range from 500 to 600 °C. The total resistance evaluated from complex impedance plan plots was observed to get a maximum value when measured at 600 °C. Further researches are in progress to explain the PTCR effect.

Acknowledgements This study is supported by the National Basic Research Program of China (2009CB623306), the International Science & Technology Cooperation Program of China (2010DFR50480), the National Nature Science Foundation of China (Grant No.50872107 and No.10875095).

References

1. Irvine JTS, Sinclair DC, West AR (1990) Adv Mater 2:132
2. Sinclair DC, West AR (1988) J Mater Sci Lett 7:823. doi: 10.1007/BF00723773
3. Dwivedi RK, Kumar D, Parkash O (2001) J Mater Sci 36:3657. doi:10.1023/A:1017997027312
4. Hirose N, West AR (1996) J Am Ceram Soc 79:1633
5. West AR, Sinclair DC, Hirose N (1997) J Electroceram 1:65
6. Sinclair DC, West AR (1989) J Appl Phys 66:3850
7. Pradhan DK, Samantaray BK, Choudhary RNP, Thakur AK (2005) J Mater Sci 40:5419. doi:10.1007/s10853-005-2824-8
8. Suman CK, Prasad K, Choudhary RNP (2006) J Mater Sci 41:369. doi:10.1007/s10853-005-2620-5
9. Nobre MAL, Lanfredi S (2003) Mater Res 6:151
10. Lily, Kumari K, Prasad K, Yadav KL (2007) J Mater Sci 42:6252. doi:10.1007/s10853-006-0824-y
11. Mahato DK, Dutta A, Sinha TP (2010) J Mater Sci 45:6757. doi: 10.1007/s10853-010-4771-2
12. Yan HX, Ning HP, Kan YM, Wang PL, Reece MJ (2009) J Am Ceram Soc 92:2270
13. Ning HP, Yan HX, Reece MJ (2010) J Am Ceram Soc 93:1409
14. Yamamoto JK, Bhalla AS (1991) J Appl Phys 70:4469
15. Satoshi N, Msakazu K, Tsutomu K (1975) J Phys Soc Japan 38:817
16. Lichtenberg F, Hermberger A, Wiedenmann K (2008) Prog Solid State Chem 36:253
17. Lichtenberg F, Hermberger A, Wiedenmann K, Mannhart J (2001) Prog Solid State Chem 29:1
18. Titov YA, Sych AM, Kapshuk AA, Yashchuk VP (2001) Inorg Mater 37:294
19. Titov YA, Sych AM, Markiv VY, Belyavina NM, Kapshuk AA, Yashchuk VP (2001) J Alloys Compd 316:309
20. Batoo KM, Kumar S, Lee CG, Alimuddin (2009) J Alloys Compd 480:596
21. Ponpandian N, Balaya P, Narayanasamy A (2002) J. Phys: Condens Matter 14:3221
22. Sivakumar N, Narayanasamy A (2007) J Appl Phys 102:013916
23. Brahma S, Choudhary RNP, Thakur AK (2005) Physica B 355:188